

Boundary layer development and summer circulation in Southern Portugal

R. Salgado¹, P. M. A. Miranda², P. Lacarrère³ and J. Noilhan³

¹Instituto de Ciências da Terra, Universidade de Évora, Portugal

²Instituto Dom Luiz, Universidade de Lisboa, Portugal

³CNRM-GAME, Météo-France, France

Received: 15-VII-2015 – Accepted: 04-XII-2015 – **Original version**

Correspondence to: rsal@uevora.pt

Abstract

The summer circulation in Southwest Iberia is studied using data from a field experiment and numerical simulations by the non-hydrostatic mesoscale model, Meso-NH. The model is initialized and forced by the ARPEGE numerical weather prediction model. Surface fields and parameters were obtained from a number of different sources and validated against observations and long period integrations of the land surface model. The numerical simulations capture most of the features found in surface and upper air observations, indicating the importance of the sea-breeze circulation in the diurnal cycle of the atmospheric boundary layer in regions more than 100 km away from the coast. The 3D nature of the summer atmospheric circulation over south Portugal is examined using results from a real case simulation of two typical summer days. Budget analyses in the 3D model are also shown, and used to clarify the relative importance of turbulent fluxes and horizontal advection in the dynamics of the boundary layer.

This article was written in 2001. For various reasons it was never published, even though part of its content is published in Portuguese in the first author's PhD thesis, defended in 2006. The work was performed using an old version of Meso-NH, but we are convinced that its main results are up to date, which justifies its publication in English in an international scientific journal. Meanwhile, one of the authors, Joel Noilhan passed away too soon. The publication of this manuscript is also a small tribute to Joel and his scientific legacy.

Key words: Sea breeze, Meso-NH, mesoscale circulations, Portugal, CICLUS

1 Introduction

The summer synoptic circulations over Iberia are basically determined by the location, intensity and shape of the Azores anticyclone and by the existence, location and intensity of the Iberian thermal low. The average surface pressure distribution (Gaertner et al., 1993, Figure 3) shows the great extent of the Azores high-pressure system, usually centered over the Azores Islands and extending in ridge throughout Central Europe. At an altitude of above 850 hPa, the pressure field is not significantly disturbed by the shallow Iberian thermal low and the region is under the influence of the anticyclone. The circulation associated with these systems creates a subsidence inversion at the top of the boundary layer (BL), where the upward expansion induced by the

BL convection and the low level convergence reinforce the anticyclonic divergence.

Thermal lows are a prominent climatological feature of many arid land areas during the warmer months, especially in low latitudes. In Europe, the Iberian Peninsula is the only place where such a system develops, acquiring a quasi-permanent character in summer (Linés, 1977; Font, 1983). The thermal low system may then be seen as the regional-scale organization of thermally driven sea breeze and valley-mountain circulations.

The Iberian thermal lows are visible in climatological analyses from late spring through the summer (e.g. Petterssen, 1956; Lefevre and Nielson-Gammon, 1995; Trigo et al., 1999). Heat lows are shallow disturbances, generally confined below 700 hPa. Using the ECMWF analyses,



Portela and Castro (1996) showed that the Iberian low is shallower still. In more than 50% of the cases, the vertical extent of the thermal low is confined below 750 hPa.

The formation of the thermal low reinforces the atmospheric convergence of surface winds from the coast. Under the sea breeze system, the maritime air masses penetrate towards the interior of the Peninsula. Their inflow has been documented as reaching more than 100 km inland from the coast (Millán et al., 1991).

According to Font (1983), Southern Portugal includes a narrow (10 to 20 km) maritime region on the western coast. To the East, up to about 100 km inland, the Atlantic influence becomes weaker and the climate may be defined as 'semi-maritime'. The climate of the eastern part is clearly continental. A large fraction of the region may be characterized as semi-arid and there is very little rainfall during summer. In the 1961-1990 period the average accumulated precipitation in JJA is of about 30 mm, with only 3 mm in August (Salgado, 1996).

An important characteristic of semi-arid regions is the fact that they are frequent candidates for significant changes in land use, including irrigation projects and the establishment of the associated water reservoirs. This is indeed the case in southern Portugal, where a large dam, Alqueva, was built to irrigate an area of about 1500 km². The impact of those interventions on the local climate has been recognized for some time (e.g. Arritt, 1984; Pielke et al., 1999) and there is a possibility that feedbacks between the mesoscale circulations forced by the modified surface and the surface fluxes of latent and sensible heat, can lead to changes in the surface water budget, cloud cover or even in convective precipitation. A good understanding of the interactions between the boundary layer development and the regional circulation is a requirement for any study on climate change induced by changes in land use. This is the main objective of the present study.

To better characterize the PBL structure and dynamics, an observational field campaign was conducted in the region: the CICLUS Experiment (Climate Impact of Changes in Land Use). The experiment included an intensive period with radiosonde observations between 16 and 31 July 1998. Data from this experiment, briefly explained in Section 2, were used to validate the mesoscale simulations.

The numerical simulations were performed with the non-hydrostatic MesoNH model (Lafore et al., 1998), briefly described in Section 3. A 48-h real case 3D simulation, at a resolution of 5 km was performed for 24 and 25 July 1998. The results are shown, in Section 4, and compared with CICLUS observations. Several analysis tools were applied, namely a budget analysis of the different terms of the evolution equations and the computation of several advective pathways.

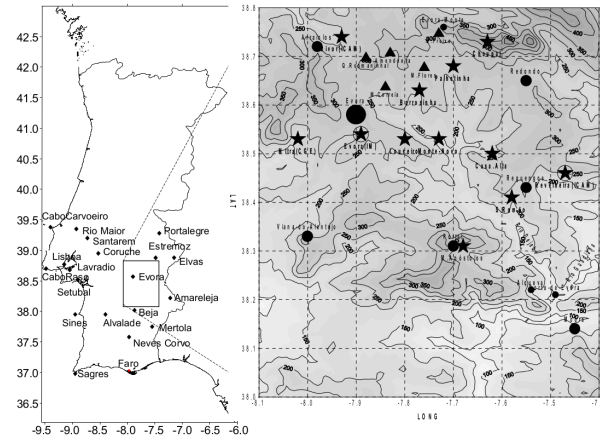


Figure 1. Left: Network of operational automatic weather stations in southern Portugal. Right: Weather stations deployed for CICLUS in the Dejebe Valley and orography at contour intervals of 50 m - (dots) Towns, (stars) weather stations; (empty dots) Radiosonde launch sites; (triangles) Automatic rain-gauges.

2 The CICLUS Experiment

The CICLUS field experiment was performed between October 1997 and September 1999, in the framework of a project developed by a team that included researchers from the Geophysics Center of the University of Évora (now ICT), the Faculty of Sciences and Technology, the Institute of Agronomy and the Institute of Meteorology (now IPMA), coordinated by Pedro M. A. Miranda, from the Geophysical Center of the University of Lisbon (now IDL). Briefly, it has included two years of continuous surface observations provided by 12 automatic weather stations and 4 extra rain gauges, installed at the Dejebe Valley, Alentejo, South Portugal. The data from the network of operational automatic stations (belonging to the Portuguese Institute of Meteorology) installed in South Portugal were also archived in the CICLUS database. Figure 1 shows the operational network and the location of the CICLUS full stations and rain gauges.

In the 12 CICLUS stations, meteorological variables (precipitation, 2-m air temperature and humidity, wind speed and direction at 2.5 m or 6 m) were monitored on a 1- to 10-minute basis. In addition, surface and sub-surface temperatures were measured in 8 stations, solar and net radiation in 7 and ground heat flux in 8. In 6 of these stations a second level of temperature and wind speed was available for indirect sensible heat flux calculation. Atmospheric pressure was measured only at the operational stations. Soil samples were occasionally collected and analysed for the moisture content at different ground levels. A rather more complete description may be found in Barroso et al. (2000).

Between 16 and 31 July 1998, an intensive field campaign was performed, including radiosondes and an eddy correlation system, consisted of an ultrasonic anemometer

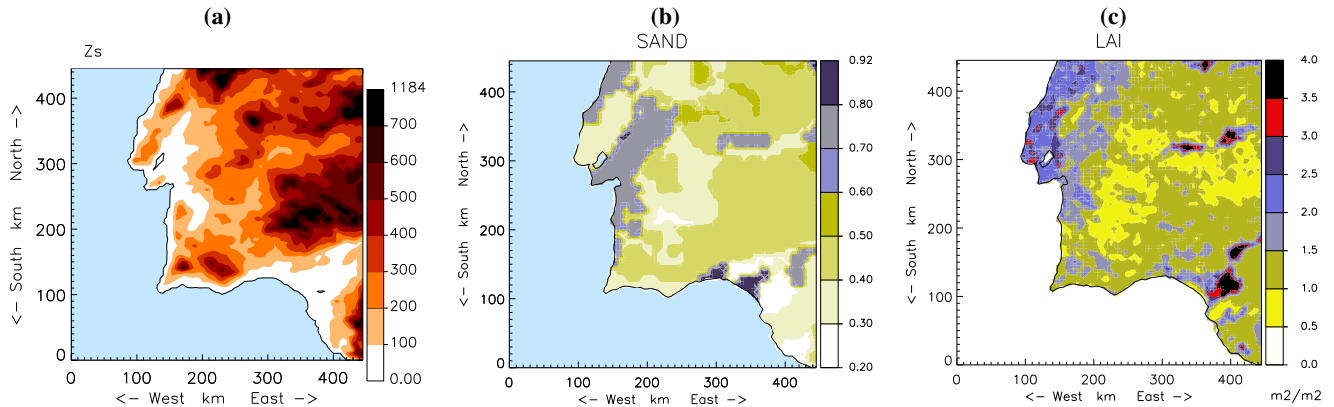


Figure 2. Horizontal simulation domain (450 km \times 450 km) and (a) orography, at contour intervals of 100 m, (b) Sand fraction (%), (c) Leaf Area Index, LAI ($\text{m}^2 \text{m}^{-2}$).

(Metek, model USA-1) and an open path krypton hygrometer (Campbell Scientific, model KH20). The radiosondes (Vaisala model RS80-15N) were launched 3 times a day (at 6, 12 and 18 UTC) from the Regional Meteorological Center of Évora (Evora IM radiosonde launch site in Figure 1) and the turbulence sensor was operated continuously. For a better understanding of the atmospheric BL evolution, during the 24 and 25 July, the radiosondes were launched every 3 hours. The last two days, intensive observation period (IOP) was chosen because it corresponds to a cloudless anticyclonic period, with low wind speed close to the surface, a common situation in the region during summertime and when local effects on the atmospheric structure and circulations are expected to be more visible.

3 The Meso-NH model and the experimental design

3.1 The Meso-NH mesoscale model

Meso-NH is a mesoscale atmospheric model developed at the *Centre National de Recherches Météorologiques* (Météo-France) and the *Laboratoire d'Aérodologie* (CNRS, France). A description of the model may be found in Lafore et al. (1998). The physical package includes a wide range of processes and several different schemes. In the present work, the following options were chosen: a Kessler (1969) type warm microphysical scheme; the Cuxart et al. (2000) turbulence scheme based on Turbulent Kinetic Energy (TKE) evolution and Bougeault and Lacarrère (1989) mixing length; a sub-grid condensation scheme based on Sommeria and Deardorff (1977); a convection scheme based on Kain and Fritsch (1990); the Fouquart-Morcrette radiation code (Morcrette, 1989).

The Interaction Soil-Biosphere-Atmosphere (ISBA) surface scheme by Noilhan and Planton (1989) was used over land surfaces. Based on the force-restore technique,

this model includes a simplified representation of vegetation. It is assumed that soil and vegetation are homogeneously mixed in each grid box. Therefore, it considers the following averaged prognostic variables: the surface and mean temperature of the soil, respectively T_s and T_2 , the near-surface and deep soil volumetric moisture content, w_g and w_2 (in $\text{m}^3 \text{m}^{-3}$), and the water intercepted by the foliage, W_r . Currently, ISBA requires the following parameters: albedo, α , emissivity, ϵ , vegetation fraction, veg , leaf area index, LAI, minimal stomatal resistance R_{smin} , percentage of clay, X_{clay} , and of sand, X_{sand} , momentum and thermal roughness lengths (z_0 and z_{0H}) and soil depth, d_2 .

The surface fluxes are computed for each land occupation type (sea, inland water, natural and cultivated land, towns) using the appropriate scheme, and then averaged in the atmospheric model grid mesh.

3.2 Experimental design

The days for CICALUS intensive observations (24 and 25 July 1998) were selected, as they represent typical summer conditions. On the 24 July 1998, the Azores Anticyclone extended in ridge, at the surface, from the West Atlantic to Central Europe, showing several high centers, namely near the western coast of Ireland and over Germany. At low levels, the Iberian thermal low, located over the south of the Peninsula, is visible in the synoptic charts (not shown). This situation is similar to the one described by Font (1983) as the most frequent summer (July and August) synoptic situation. Over the region of study, the low-level flow is characterized by weak to moderate northerly winds. Above 850 hPa, west-southwesterly winds prevail.

The horizontal simulation domain of the 3D simulation (Figure 2) was covered by a mesh of 90×90 grid elements, with a resolution of $5 \times 5 \text{ km}^2$. The domain included the southwestern sector of the Iberian Peninsula and many points over the Atlantic Ocean, in order to keep the boundaries

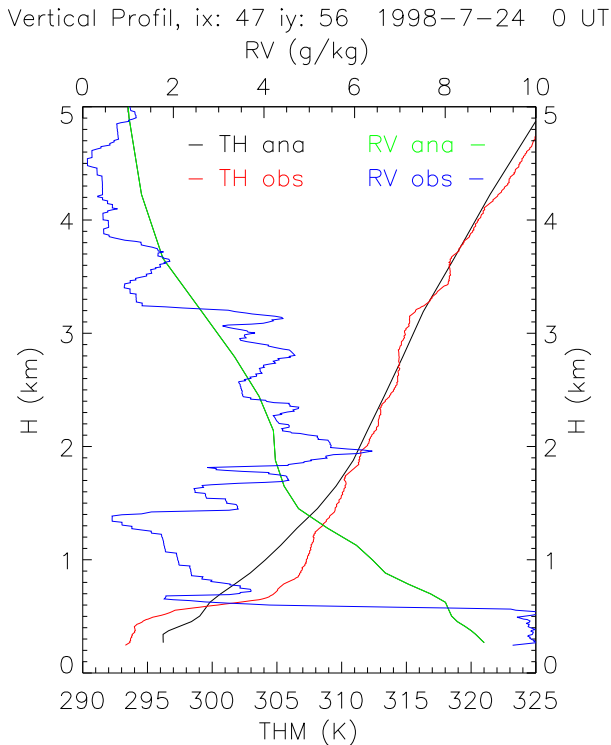


Figure 3. Vertical profiles of potential temperature (TH) and mixing ratio (RV) over Évora on 24 July 00 UTC: observed (obs) and analyzed (ana) profiles.

sufficiently away from the region of main interest and to provide this region with maritime advection, expected to be important in the establishment of the observed circulation. In the vertical, 40 levels were considered from the surface up to about 20 km, mostly distributed in the low troposphere (20 levels in the first 2 km). The lowest thermodynamic level is at approximately 10 m above ground level. The model ran for 48 hours, starting at 0000 UTC on the 24, with a 20-s time step.

3.3 Physiographic data

The GTOPO30 database at a 30 arc-second horizontal resolution, from the U.S. Geological Survey, was used to generate the orography map (Figure 2a).

The CORINE land cover 1:100 000 database (EEA, 1993) was used to mask the land, sea, inland water and urban fractions. CORINE land cover consists of a European geographical database describing land cover forms in 44 classes, considering both physical and physiognomic characteristics.

Soil texture and depth maps were computed from the FAO Digital Soil Global Maps at a resolution of 5 arc-minute by 5 arc-minute units and a set of composition rules defined in FAO (1978), as described in Salgado (1999). The textural information was converted to the variables used as input parameters by the soil model: X_{clay} and X_{sand} , the clay and

sand fractions (Figure 2b), and soil depth, d_2 .

To generate the maps of vegetation-dependent parameters, the AVHRR-derived vegetation map produced by Champeaux et al. (2000), based on 10 years of NDVI (Normalized Difference Vegetation Index), was used. ISBA vegetation parameters were associated with this vegetation map, taking into account its seasonality, leading to (climatological) monthly maps of LAI, veg, R_{smin} , and vegetation contributions to z_0 , α and ϵ .

The aggregation to the model domain resolution was made following Noilhan and Lacarrère (1995). LAI values around $1 \text{ m}^2 \text{ m}^{-2}$ (Figure 2c) and veg values of about 0.5 (not shown) are found over the CICLUS region, which are consistent with the semi arid character of the region.

3.4 Initial and coupling fields

The initial and coupling fields were obtained from the ARPEGE (French operational weather forecast model) analysis corresponding to 0, 6, 12, 18 UTC on 24 and 25 July 1998, which uses the same land-surface parametrization ISBA scheme used by Meso-NH. The surface prognostic variables (T_s , T_2 , w_g , w_2 , W_r) were initialized using the surface optimum interpolation algorithm described in Giard and Bazile (2000). In the region where the CICLUS field campaign was performed, the values of w_g lie between 0.09 and $0.13 \text{ m}^3 \text{ m}^{-3}$ and w_2 between 0.15 and $0.20 \text{ m}^3 \text{ m}^{-3}$, in general slightly below the wilting point (the minimal point of soil moisture the plant requires not to wilt). These values correspond to those measured in collected soil samples at the sites referred to in Table 1 and shown on Figure 1.

The comparison (not shown) between the initial temperature and humidity fields interpolated to 2 m, using Monin-Obuhkov similarity laws, and the screen-level observations at the surface synoptic network, show that the analysis overestimated temperature and underestimated relative humidity over land. The differences in temperature are of the order of 5 K at some points. On the other hand, above the surface BL, the analyzed values coincide well with the observed ones, as shown by the vertical profiles over the city of Évora represented in Figure 3. The differences at low-levels are due to an insufficient representation of the nocturnal cooling of the surface layer in the ARPEGE analysis, which will eventually be corrected during the Meso-NH simulations.

4 Results from 3D Simulations

4.1 Near surface meteorological variables

The 3D simulation results were compared with the observational data. The evolution of the spatial patterns of both predicted temperature and relative humidity at screen-level coincide with those measured by the surface network

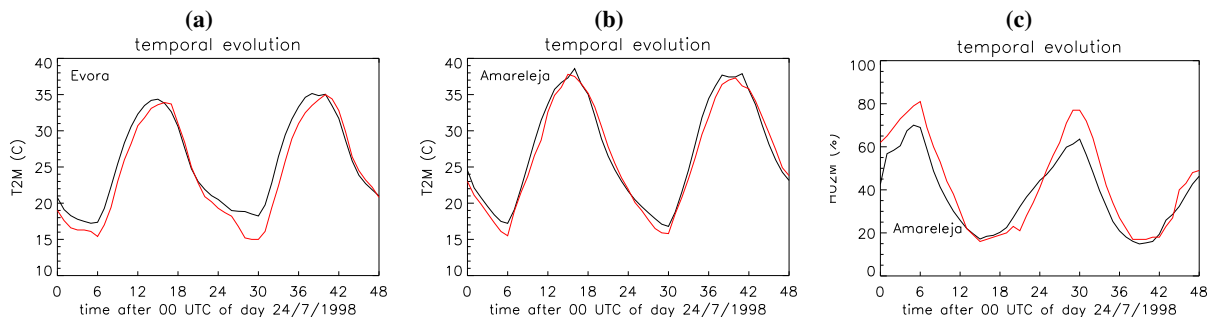


Figure 4. Temporal evolution of the 2 m air temperature (° C) in (a) Évora and (b) Amareleja and (c) 2 m relative humidity (%) in Amareleja. Simulated values in black and observations in red.

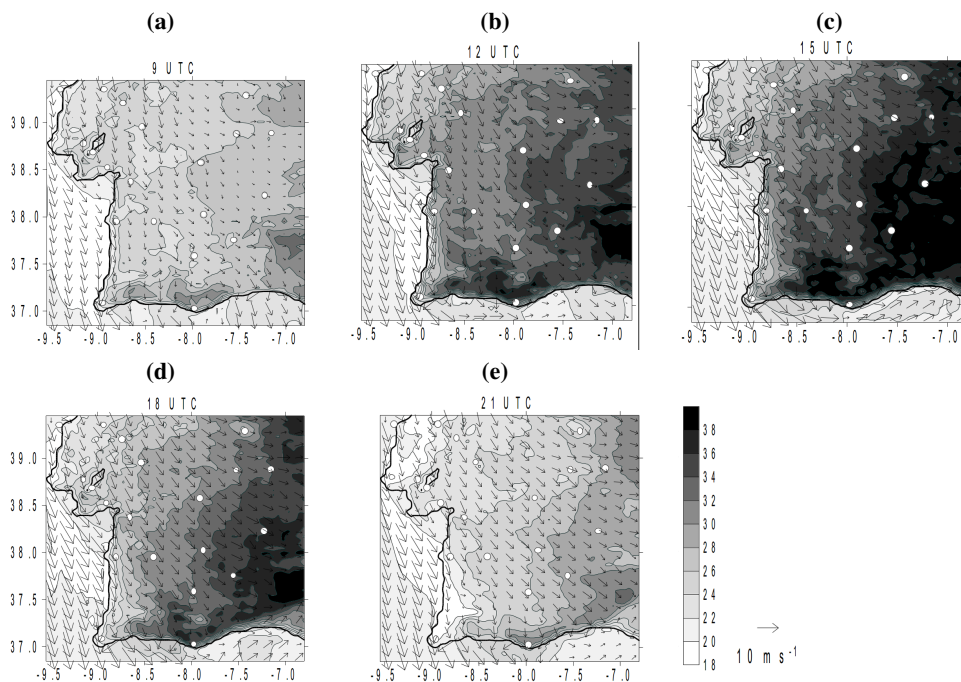


Figure 5. Screen level maps of simulated temperature and wind at 09, 12, 15, 18 and 21 UTC on 24 July 1998. Vertical axis in degrees of latitude and horizontal axis in degrees of longitude.

Table 1. Measurements of soil volumetric water content at some experimental sites on 23 July 1998. Soil samples from two layers have been collected and analyzed.

Site	Water content ($\text{m}^3 \text{m}^{-3}$)	
	0-0.1 m layer	0.1-0.4 m layer
Palhetinha (38.67 N; 7.70 W)	0.13	0.17
Casa Alta (38.50 N; 7.62 W)	0.11	0.12
Choupal (38.73 N; 7.63 W)	0.10	0.11
Barrosinha (38.63 N; 7.77 W)	0.15	0.21

(Figure 4 for selected locations). In spite of the differences that subsist early in the morning, as a consequence of the above-mentioned initial overestimation of temperature (Section 3.4) and underestimation of humidity, the model is

able to reproduce the diurnal cycle. Elsewhere, there is a good match between simulations and observations. At 15 and 18 UTC, in all inland stations, the differences between observed and simulated values are smaller than 2 K. The model 2 m temperature bias lies between -0.5 and 1.8 K, with an average value (over all synoptic stations) of 0.75 K. At the coastal stations, the large horizontal temperature gradients (up to 1 K km^{-1}) make the comparison rather difficult, but if one takes the best simulated value over a square windows ($5 \text{ km} \times 5 \text{ km}$) surrounding the observation points, the errors are of the same order of magnitude as in inland stations.

Model results identify the valleys of the Guadiana and Guadalquivir rivers as the areas of highest values of the maximum daily temperature (see Figure 5). Most of the tem-

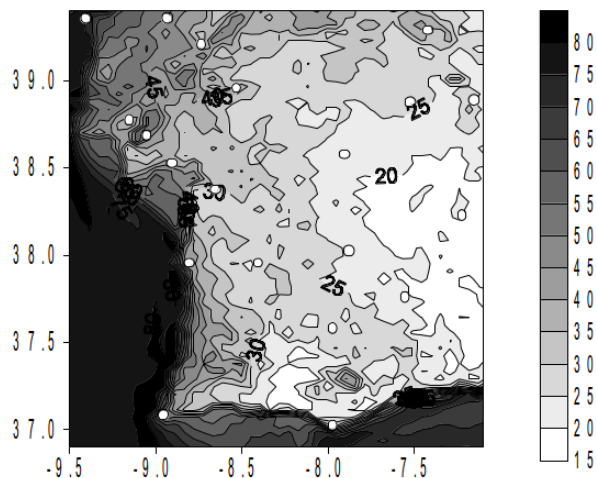


Figure 6. Simulated screen level relative humidity (in %) at 15 UTC. Vertical axis in degrees of latitude and horizontal axis in degrees of longitude. White dots indicate the location of the stations belonging to the surface network.

perature gradient is along the west-east direction, associated with the horizontal advection of cooler Atlantic air, by the sea breeze circulation, mainly aligned in the northwesterly direction, but which is blocked by the mountain ridge close to the southern Portuguese coast. For this reason, and also because the northwesterly wind regime implies downslope isentropic subsidence in the lee side of the mountain ridge, maximum temperatures at the southern edge of Portugal (the Algarve) are comparable with those found in interior locations.

The simulated wind field, also shown in Figure 5, is also a good match with observations. As observed, the wind is northwesterly everywhere, except in the Northeast sector of the domain, where it is very weak in the morning and westerly in the afternoon. The comparison between the near surface wind field and pressure distributions reveals the existence of an ageostrophic wind component, converging to the interior of the Iberian Peninsula. Both observations and simulations show an intensification of the wind in the warmer hours, with the maximum wind speed attained at the end of the afternoon.

The importance of the advection of maritime air is very clear in the evolution of surface temperature distribution. That advection is forced by the northwesterly circulation associated with the thermal low, and reinforced by the diurnal cycle of the sea breeze. The sea breeze circulation is easily spotted by the increase in the westerly component of the wind in all locations close to the west coast and by the rotation of the wind vector on the south coast, to southwesterly. The effect is observed in many stations at up to 100 km from the coast. At Évora, about 80 km inland, observations show evidence of sea breeze effects at about 18 UTC.

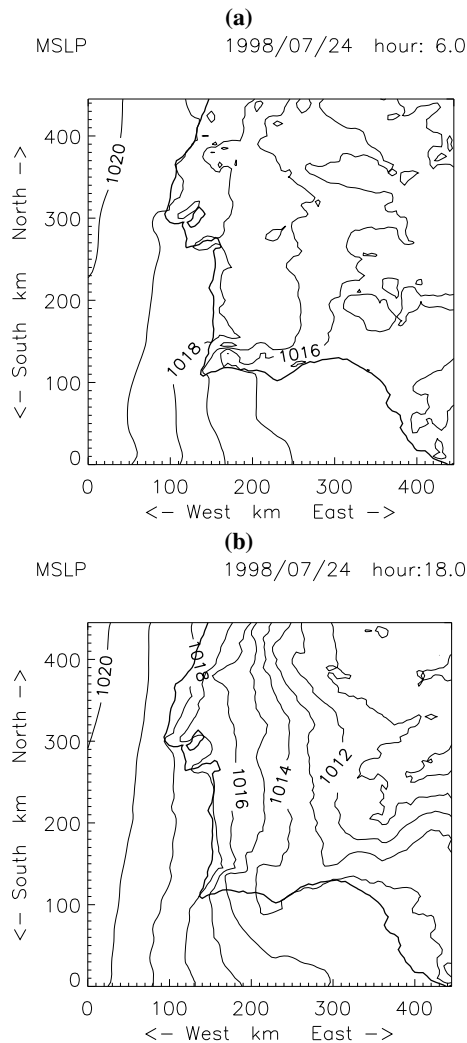


Figure 7. Simulated mean sea level pressure at 6 and 18 UTC, on 24 July 1998.

The intensification of the sea breeze circulations is partially explained by a superposition with an upslope wind circulation, generated, during day time, in all near coastal slopes. In some places, such as near the southwestern corner of Iberia, the superposition of those effects explains lower values of maximum temperature.

The simulated air relative humidity at screen level, at 15 UTC, is shown in Figure 6. Despite the underestimation overnight, during the warmer hours of the day, there is a good match between simulations and observations, with minimum relative humidity values below 20% in the driest sector, to the east of the domain, similar to those measured in Amareleja (Figure 4c). Due to the presence of the Iberian thermal low, the minimum of mean-sea-level (SL) pressure is always found at the most interior part of the domain (Figure 7). This minimum attains its diurnal maximum (minimum) approximately at 06 UTC (18 UTC), when the thermal low is weakest (strongest). Between 06 UTC

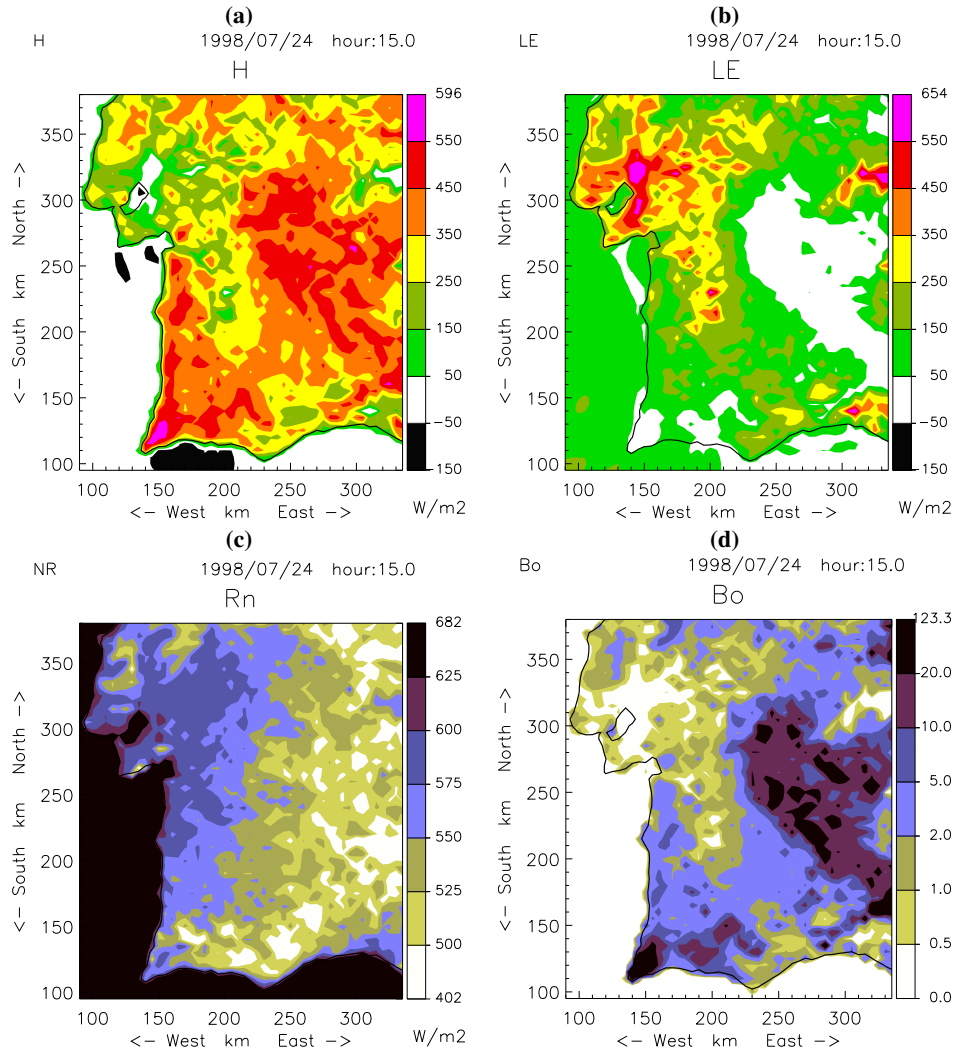


Figure 8. Surface fluxes in 3D simulation, at 15 UTC 24 July 1998: (H) Sensible heat flux and (LE) Latent heat flux, both with contour intervals of 100 W m^{-2} ; (R_n) Net Radiation over land surfaces (contour intervals of 25 W m^{-2}); (Bo) Bowen ratio (irregularly spaced contour levels).

and 18 UTC the SL pressure decreases by about 4 hPa in this region. In the morning, the isobars are aligned in a north-south direction, while in the afternoon they are almost parallel to the coastlines and the pressure gradients are more intense near the west coast. These results correspond to those showed by Portela and Castro (1996).

4.2 Surface fluxes

The existence of regions with relative high air temperatures and very low values of relative humidity, showed in the previous section, are a direct consequence of the existence of a strong sensible heat flux from the surface into the atmosphere. This fact is visible in Figure 8, where the surface fluxes of latent (LE) and sensible (H) heat at 15 UTC 24 July are shown. Over land grid points, where the fraction

of inland waters is almost zero, H is, in general, greater than 250 W m^{-2} and attains a maximum value close to 600 W m^{-2} . In the areas where H is larger, LE is very low, near zero, leading to Bowen ratio (Bo) values of greater than 10 (Figure 8). Those areas, where there is virtually no evaporation, are found in the interior and near the southeast corner. Furthermore, areas where Bo is lower than 1 are mostly distributed along the north edge of the simulation domain (close to the Tagus valley). The map of simulated Net Radiation (R_N) at the surface (Figure 8) shows a west-west gradient, related to the surface temperature gradient. Values greater than 600 W m^{-2} are simulated near the west coast, while in the interior R_N is close to 500 W m^{-2} .

A more detailed analysis of the time evolution of surface fluxes is shown in Figure 9, comparing eddy-correlation estimations of latent and sensible heat fluxes with model grid point values of those variables. It is clear that the

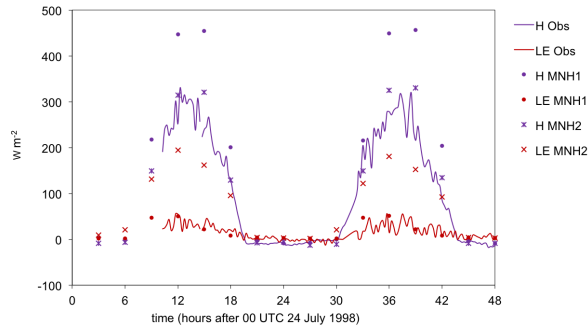


Figure 9. Comparison between observed and simulated diurnal evolution of surface sensible (H) and latent (LE) heat fluxes. Observation values (Obs) were measured with the eddy correlation system installed at Louseiro. Simulated values over the grid point corresponding to the location of the Louseiro station (MNH1) and 4 grid points (20 km) to the west (MNH2).

energy partition in the model varies substantially between nearby grid points, but model values are comparable with observations. The total convective fluxes (LE + H) are, though, somewhat larger in the model, around 30%. Eddy correlation systems are expected to underestimate surface fluxes in convective conditions, due to both the limits of their spectral windows and of the local closure assumption.

4.3 Vertical profiles

The development of an unstable convective BL is the first atmospheric response to strong sensible heat fluxes, at the surface over land. The evolution of the potential temperature over the point corresponding to the site of Évora (Figure 10), shows that the model reproduces the BL diurnal thermal structure very well, namely its depth. The 5-km non-hydrostatic simulation is qualitatively closer to the observations than the large-scale analysis. The model run did not reproduce the thermal structure of the nocturnal surface layer (from ground up to 300 m) with the same accuracy.

On the first day of simulation, the BL depth reached a maximum value of about 1300 m, approximately at 15 UTC. At the same time on day 2, the BL top attained 1600 m. In both situations, the BL was well mixed with a constant potential temperature of 305 K on day 1 and 306 K on day 2. After 15 UTC the average temperature of the BL decreases slightly while its depth decreased. During the 16 days of the CICALUS campaign, the maximum BL depth varied between 1000 and 2500 m, and its average maximum potential temperature between 298 K (20 July) and 312 K (28 July).

The evolution of the mixing ratio profiles (not shown) also confirms the ability of Meso-NH to represent the observed PBL. The observed profiles show a very dry layer above the BL top, capped by a relatively moister layer. This

feature is found on both days, and in other profiles during the CICALUS campaign, but it is not captured by the large-scale analysis, and therefore is not present in the initial Meso-NH fields. The Meso-NH profiles tend to correspond to the observed ones in a quite reasonable manner, indicating that some of the relevant dynamics are present in the model.

The 3D simulation reproduces the main characteristics of the evolution of wind direction over Évora (not shown), namely its diurnal rotation from northerly in the night and early morning to northwesterly in the afternoon. The intensification of the low-level wind speed at night was also well predicted, namely the formation of the nocturnal jet. On both days, there is a clear reversal of the zonal wind component at low-levels at about 15 UTC, when it becomes positive (from west) and accelerates until 18 UTC, indicating the arrival of the sea breeze.

4.4 Vertical structure

Figure 11 shows south-north and west-east cross-sections of water vapor mixing ratio and normal wind, which help to visualize the 3D circulation. The two cross-sections intersect in a vertical profile corresponding to the Évora radiosonde site. The W-E cross-section shows a clear signature of the thermal low, centered to the east of Évora, in the meridional component of the wind: northerly in the west sector and easterly in the east sector. The structure of the humidity field looks very much like a 3D plume, with a region of maximum moisture linking coastal air, at low levels, with a moister layer above the BL. The structure of that plume is an indication of the complex circulation generated by the interaction of the converging sea-breeze at low levels with the large scale subsidence in the mid troposphere. The complicated structure of the humidity field just above the BL is related with the different origins of air parcels arriving at a given profile.

4.5 Budget analysis

A budget analysis was performed at the CICALUS central site, based on the model equations and consisting in of 15-min temporal averaging of all the forcing terms considered in the prognostic equations of θ and r_v . The averaging process was applied each hour between 6 UTC and 20 UTC on the 24 July.

Ignoring the terms associated with phase changes, which did not occur, the forcing terms in the thermodynamic equation are the grid scale transport (advection), the sub-grid flux (turbulence) and the radiative heat flux. During daytime, except in the first 100/150 m above the surface, only the advective and the turbulent terms are significant. The evolution of these two terms is shown in Figure 12. Advection and turbulence are, generally, in opposite phase: in the BL, the advective flux is negative, except between 6 and 7 UTC, whereas the turbulent flux is always positive.

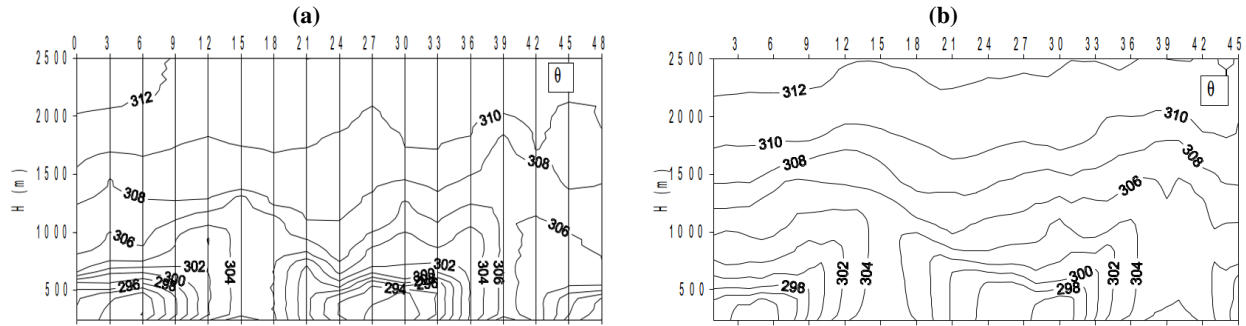


Figure 10. Height(H)-time cross-sections of (a) observed and (b) simulated potential temperature (θ) over Évora. Observed values were interpolated from the radiosondes launched at Évora every 3 hours (grid-lines in (a)). Height in m above mean-sea-level and time in hours after 00 UTC of 24 July 1998.

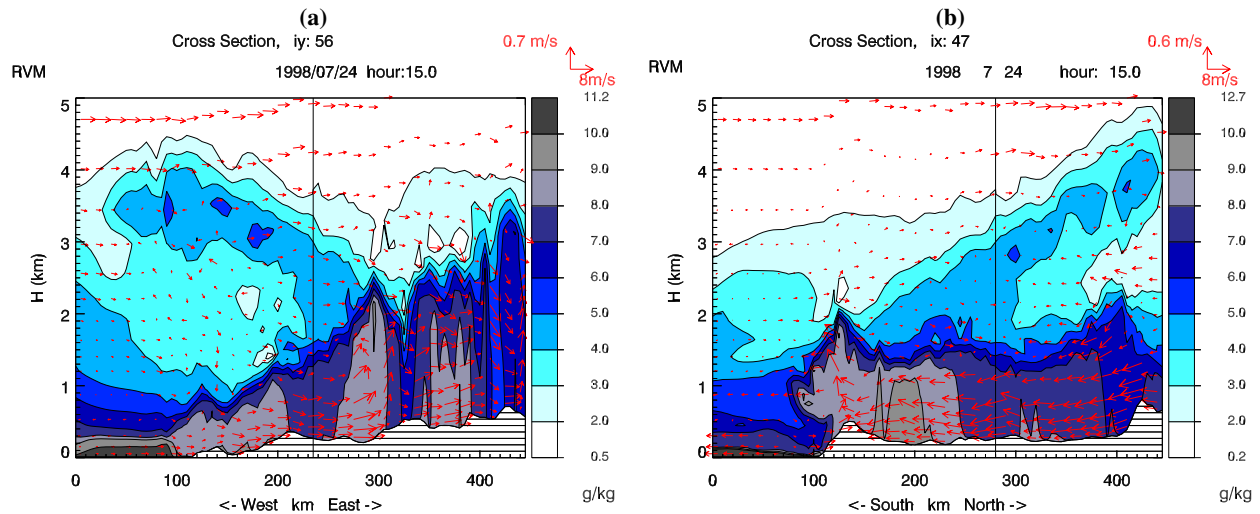


Figure 11. Results from 3D simulation: S-N (b) and W-E (a) cross sections at 15 UTC of the mixing ratio (in g kg^{-1} , with Contour intervals of 0.5) and wind parallel to the considered planes (arrows). H is the height above mean-sea-level in km.

In the morning, the turbulent flux dominates and induces the development of the BL, attaining a maximum at 11/12 UTC, while in the afternoon, after 16 UTC, the advective flux becomes higher in module, cooling the well-mixed BL as a whole. As θ is almost constant with respect to height within the BL, the advective cooling is due to the sea breeze horizontal advection of maritime air. Above the BL, there is a layer where the advection of θ is positive and the turbulent flux is negative, due to entrainment of warm air down to the BL. In the morning, the two terms cancel, but in the afternoon, advection becomes dominant, heating the layer and “pushing down” the top of the BL. Here, the advective flux is mostly vertical, related to large-scale subsidence.

In the absence of phase changes, the evolution of r_v is forced only by advective and turbulent fluxes. The advection term (Figure 13) was the most relevant term. During the morning, in the BL, the grid scale flow transported dry air from the northeast into the column. After 16 UTC, the

advective flux was positive in the BL, corresponding to the arrival of the sea breeze, bringing moister air. Immediately above the top of the BL, the advective flux is strongly negative after midday. Although it is partially compensated by a positive turbulent flux, the horizontal advection of dryer air is responsible for the establishment of the narrow dryer layer, shown in the observed profiles (e.g. Figure 3). Close to an altitude of 4 km, the r_v advective flux is always positive, inducing the establishment of a moister layer.

5 Conclusions

This study used data obtained in a field experiment performed in south Portugal and the Meso-NH modeling system to study the summer circulation on the Iberian Peninsula. The Meso-NH model, was found to be able to reproduce the main features of the observed circulation and the diurnal

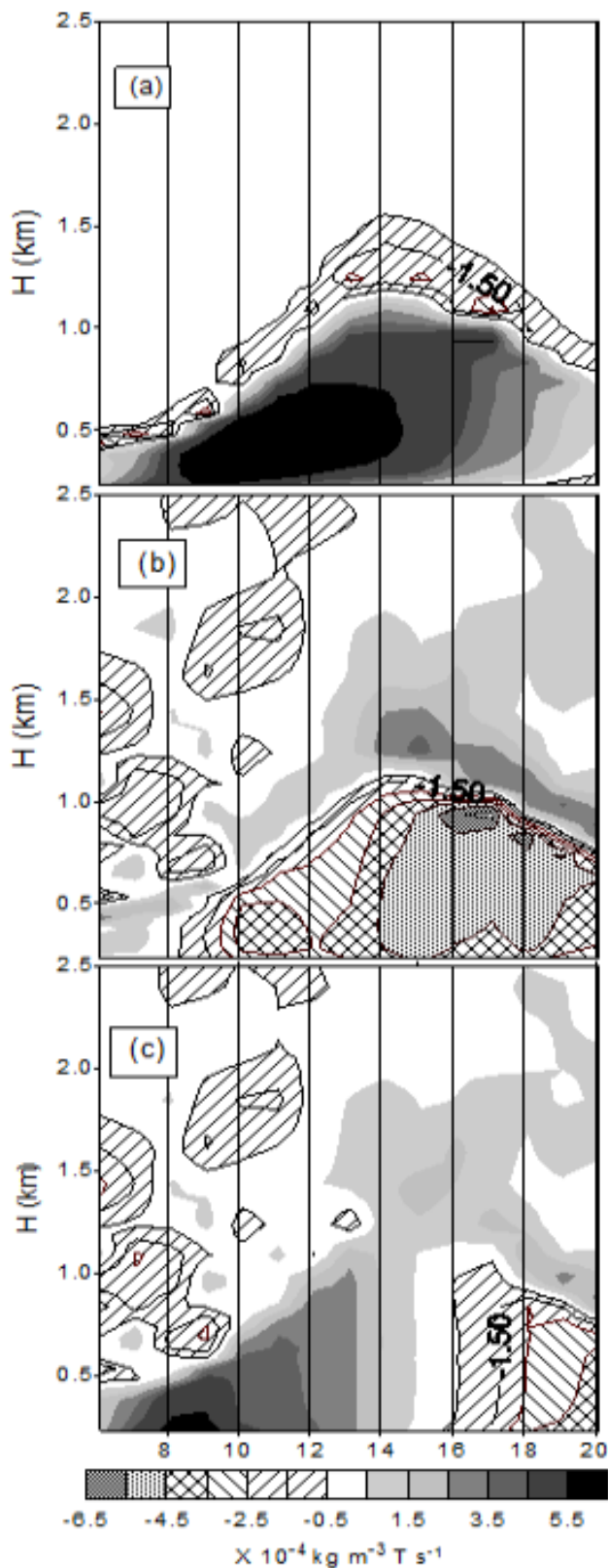


Figure 12. Height(H)-time cross sections of the evolution of the forcing terms in the thermodynamic equation: (a) advective flux, (b) turbulent flux, (c) sum of all forcing terms (advective, turbulent and radiative). Horizontal axis in hours after 00 UTC of 24 July 1998.

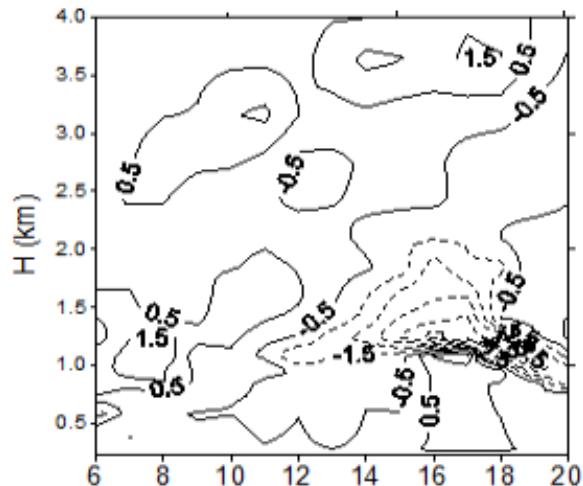


Figure 13. Height(H)-time cross sections of the evolution of the advective flux in the *rv* prognostic equation (units $10^{-7} \text{ kg m}^{-3} \text{ s}^{-1}$). Horizontal axis in hours after 00 UTC of 24 July 1998.

evolution of the boundary layer, as observed by the operational weather network and by frequent radiosondes at the experimental site.

The analysis of the three-dimensional fields of the Meso-NH simulations has confirmed the qualitative knowledge, from meteorological forecasters, on the dynamics of the sea breeze in South Portugal. At the same time, the detail given by these simulations permits a better understanding of the dynamics and a quantification of the size of its effects.

On the Iberian Peninsula, the summer circulation generated by the land-sea thermal contrast is associated with the regional circulation of a thermal low in the central region, well away from the direct effect of the sea. The interaction between these effects at local and regional scales, tends to reinforce the special character of the Iberian circulation. The results from numerical simulations showed that the evolution of the BL in the interior of the Peninsula is strongly influenced by the horizontal transport of heat and moisture in the sea-breeze circulation, even in locations at more than 100 km from the coast, where a direct sea-breeze effect might be expected to be of reduced importance. This influence occurs in the form of a bulk cooling of the BL in mid to late afternoon, depending on the distance from the coast. The results also showed evidence of complex 3D transport of humidity in the Iberian region, linking the coastal source region with the mid troposphere where it interacts with the large-scale subsidence, associated with the anticyclonic circulation in the upper levels. The climatological importance of this transport cannot be proven from the 2 weeks of radiosondes performed, but the corresponding vertical patterns of the humidity profile were frequently observed during this period.

These conclusions were drawn in 2001. They were developed and extended in the PhD thesis of Salgado (2006,

in Portuguese). Despite not having the same purpose, further works over the same region with newer versions of Meso-NH, with improved surface schemes, currently externalized in the context of SURFEX (Masson et al., 2013), and finer resolutions do not contradict it. Examples may be found in Costa et al. (2010) in a study on the orographic precipitation over Iberia and in Santos et al. (2013) in a modeling work about Saharan desert dust transported over south Portugal. The data from the CICLUS field experiment were used in several studies, including Teixeira et al. (2004), to test a new mixing-length formulation for the parameterization of dry convection. New research is currently being conducted, using Meso-NH, to investigate the boundary layer effects of the construction of a large reservoir in the region (Alqueva). For this purpose, the representation of lakes in SURFEX was improved (Salgado and Le Moigne, 2010) by inserting the FLake model (Mironov et al., 2010) and a new field experiment, ALEX 2014 (www.alex2014.cge.uevora.pt), was carried out in summer 2014.

Acknowledgements. The first author would like to acknowledge the GMME/CNRM/Meteo-France for the facilities made available during his research stage. Special thanks to V. Masson, S. Donier and the Meso-NH team for useful comments and help in the use of computational facilities.

This study was carried out under Project CICLUS, Portuguese Science Foundation (FCT) Grant 3/3.2/EMG/1968/95. Rui Salgado had the support of FCT, under grant PRAXIS XXI/BD/15988/98.

References

- Arritt, R. A., 1984: *Enhancement of convective precipitation by mesoscale variations in vegetative covering in semiarid regions*, J. Climate Appl. Meteor., **23**, 541–554.
- Barroso, C. S. F., Miranda, P. M. A., Soares, P. M. M., Salgado, R., Cardoso, R., Rodrigues, A. C., Diogo, P., Abreu, F., Carvalho, M., Ferreira, M., Carvalho, R., Barbosa, S., Prior, V., and Nunes, L. F., 2000: The CICLUS Observational Experiment, In Proceedings of the 2^a Assembleia Luso-Espanhola de Geodesia e Geofísica, Proceedings of the 2^a Assembleia Luso-Espanhola de Geodesia e Geofísica.
- Bougeault, P. and Lacarrère, P., 1989: *Parameterization of orography-induced turbulence in a meso-beta-scale model*, Mon. Weather Rev., **117**, 1872–1890.
- Champeaux, J.-L., Arcos, D., Bazile, E., Giard, D., Goutorbe, J.-P., Habets, F., Noilhan, J., and Roujean, J.-L., 2000: *AVHRR-derived vegetation mapping over Western Europe for use in numerical weather prediction models*, International Journal of Remote Sensing, **21**, 1183–1199.
- Costa, M. J. R., Salgado, R., Santos, D., Leviazzani, V., Bortoli, D., Silva, A. M., and Pinto, P., 2010: *Modelling of orographic precipitation over Iberia: a springtime case study*, Adv. Geosci., **25**, 103–110.
- Cuxart, J., Bougeault, P., and Redelsperger, J., 2000: *A turbulence scheme allowing for mesoscale and large-eddy simulations*, Q. J. R. Meteorol. Soc., **126**, 1–30.
- EEA, 1993: CORINE Land Cover, Technical guide. EUR 1285 EN, European Environment Agency, Official Publications of the European Communities, Luxembourg, http://etc.satellus.se/the_data/Technical_Guide/index.htm.
- Font, I., 1983: *Climatología de España e Portugal*, Inst. Nac. de Meteorología, Min. Transp. y Com., Madrid.
- Gaerter, M. A., Fernández, C., and Castro, M., 1993: *A Two-dimensional simulation of the Iberian summer thermal low*, Mon. Weather Rev., **121**, 2740–2756.
- Giard, D. and Bazile, E., 2000: *Implementation of a new assimilation scheme for soil and surface variables in a global NWP model*, Mon. Wea. Rev., **128**, 997–1015.
- Kain, J. S. and Fritsch, J. M., 1990: *A one dimensional entraining/detraining plume model and its application in convective parameterization*, J. Atmos. Sci., **47**, 2784–2802.
- Kessler, E., 1969: *On the distribution and continuity of water substance in atmospheric circulations*, Meteor. Monogr., **32**.
- Lafore, J. P., Stein, J., Asencio, N., Bougeault, P., Ducrocq, V., Duron, J., Fischer, C., Hereil, P., Mascart, P., Pinty, J. P., Redelsperger, J. L., Richard, E., and de Arellano, J. V.-G., 1998: *The Meso-NH Atmospheric Simulation System. Part I: Adiabatic formulation and control simulations*, Annales Geophysicae, **16**, 90–109.
- Lefevre, R. J. and Nielsen-Gammon, J. W., 1995: *An objective climatology of mobile troughs in the Northern Hemisphere*, Tellus, **47A**, 638–655.
- Lines, A., 1977: *The climate of the Iberian Peninsula. Climates of northern and western Europe*, C. C. Wallén, Ed., World survey of Climatology, 5, Elsevier.
- Mason, P. J., 1991: *Boundary-layer parameterization in heterogeneous terrain. Workshop Proc. on Fine Scale Modelling and the Development of Parameterizations Schemes*, ECMWF, pp. 275–288.
- Mironov, D., Heise, E., Kourzeneva, E., Ritter, B., Schneider, N., and Terzhevik, A., 2010: *Implementation of the lake parameterization scheme FLake into the numerical weather prediction model COSMO*, Boreal Environ. Res., **15**, 218–230.
- Morcrette, J., 1989: *Description of the radiation scheme in the ECMWF model*, ECMWF Tech. Memo. 165, 26 pp.
- Noilhan, J. and Lacarrère, P., 1995: *CGM grid-scale evaporation from mesoscale modeling*, J. Climate, **8**, 206–223.
- Noilhan, J. and Planton, S., 1989: *A simple parameterization of land surface processes for meteorological models*, Mon. Wea. Rev., **117**, 536–549.
- Petterssen, S., 1956: *Weather Analysis and Forecasting, Vol1: Motion and Motion Systems*, McGraw-Hill, 428 pp.
- Pielke, R. A., Walko, L., Steyaert, L. T., Vidale, P. L., Liston, G. E., and Chase, T. N., 1999: *The Influence of Anthropogenic Landscape Changes on Weather in South Florida*, Mon. Wea. Rev., **127**, 1663–1673.
- Portela, A. and Castro, M., 1996: *Summer thermal lows in the Iberian peninsula: A three-dimensional simulation*, Quart. J. Roy. Meteor. Soc., **122**, 1–22.
- Salgado, R., 1996: *Modelação de circulações atmosféricas induzidas por heterogeneidades na superfície, dissertação para a obtenção do grau de Mestre em Ciências Geofísicas – Área de Meteorologia*.
- Salgado, R., 1999: *Global soil maps of sand and clay fractions and of the soil depth for MESONH simulation based on FAO/UNESCO soil maps*, CNRM/Météo France Tech., 59.

- Salgado, R., 2006: *Interacção solo - atmosfera em clima semi-árido*, Ph.D. thesis, Universidade de Évora.
- Salgado, R. and Moigne, P. L., 2010: *Coupling of the FLake model to the Surfex externalized surface model*, *Boreal Env. Res.*, **15**, 231–244.
- Santos, D., Costa, M. J., Silva, A. M., and Salgado, R., 2013: *Modeling Saharan desert dust radiative effects on clouds*, *Atmos. Res.*, **127**, 178–194.
- Sommeria, G. and Deardorff, J., 1977: *Subgrid-scale condensation in models of nonprecipitating clouds*, *J. Atmos. Sci.*, **34**, 344–355.
- Teixeira, J., Ferreira, J. P., Miranda, P. M. A., Haack, T., Doyle, J., Siebesma, A. P., and Salgado, R., 2004: *A new mixing length formulation for the parameterization of dry convection: Implementation and evaluation in a mesoscale model*, *Monthly Weather Review*, **132**, 2698–2707.
- Trigo, I. F. and Davies, T. D., 1999: *Objective climatology of cyclones in the Mediterranean region*, *J. Climate*, **12**, 1685–1696.